Seismic monitoring leveraging existing telecom infrastructure at the SDASA: Active, passive, and ambient-noise analysis

Eileen R. Martin[1], Chris M. Castillo[1], Steve Cole[2], Paphop Stock Sawasdee[1], Siyuan Yuan[1], Robert Clapp[1], Martin Karrenbach[2], and Biondo L. Biondi[1]

Abstract

We analyze active and passive seismic data recorded by the Stanford distributed acoustic sensing array (SDASA) located in conduits under the Stanford University campus. For the active data we used low-energy sources (betsy gun and sledge hammer) and recorded data using both the DAS array and 98 three-component nodes deployed along a 2D line. The joint analysis of shot profiles extracted from the two data sets shows that some surface waves and refracted events are consistently recorded by the DAS array. In areas where geophone coupling was suboptimal because of surface obstructions, DAS recordings are more coherent. In contrast, surface waves are more reliably recorded by the geophones than the DAS array. Because of the noisy environment and weak sources, neither data set shows clear reflections. We demonstrate the repeatability of DAS recordings of local earthquakes by comparing two weak events (magnitude 0.95 and 1.34) with epicenters 100 m apart that occurred only one minute from each other. Analyzing another local, and slightly stronger, earthquake (magnitude 2.0) we show how the kinematics of both the P-arrival and S-arrival can be measured from the DAS data. Interferometric analysis of passive data shows that reliable virtual-source responses can be extracted from the DAS data. We observe Rayleigh waves when correlating aligned receivers, and Love waves when correlating receivers belonging to segments of the array parallel to each other. Dispersion analysis of the virtual sources shows the expected decrease in surface-wave velocity with increasing frequency.

Introduction

Since September 2016, we have been conducting an ongoing permanent seismic recording experiment utilizing fiber-optic cables lying in PVC conduits buried in the ground under the Stanford University campus. These conduits existed prior to our experiment and are shared with other fiber cables used to support Internet traffic among Stanford's academic buildings. Coupling between the fiber cable and surrounding rocks relies exclusively on gravity and friction. Our experiment is therefore different from other experiments utilizing directly buried horizontal fiber cables. The potential cost efficiency of leveraging existing telecom infrastructure is enormous, particularly in urban and suburban areas. If successful, our experiment could enable large-scale seismic monitoring that would be otherwise impossible. The results of our experiment could also lead to the use of ad-hoc inexpensive "slim holes" above reservoirs with PVC casing buried sufficiently deep to bypass near-surface complexities and their negative effect on conventionally recorded land data.

The main goals of our experiment are: (1) to assess the quality of the recorded data, given the less-than-optimal coupling between the fiber cable and the surrounding rocks, and (2) to develop novel processing and imaging algorithms that are tailored to the unique opportunities, and deficiencies, of data recorded using the proposed setup. In particular, applications in noisy environments (either urban or oil field) together with the "streaming" nature of the data recording require new processing techniques and paradigms.

In this paper we discuss and show examples of the application of our open-conduit recording configuration to: (1) recording active data from low-energy sources, (2) passive recording of weak local seismic and microseismic events, and (3) time-lapse interferometric imaging of the near surface.

The analysis of the active distributed acoustic sensing (DAS) data benefits from the contemporaneous deployment of 98 FairfieldNodal ZLand three-component (3C) nodes since their comparison helps validate and interpret the events identified in the DAS recordings. For the passive recording we are benefiting from the uniquely suited location of the Stanford campus. We have already catalogued more than 700 seismic events that occurred in Northern California between September 2016 and July 2017; new events are recorded daily. For interferometric imaging, the Pacific Ocean is only 22 km away providing microseism energy, and major freeways run both east and west of campus generating plenty of higher frequency traffic noise.

Installation

The sensitivity of DAS to any event is more strongly influenced by directionality than single-component geophones, so our array includes fiber segments in two roughly orthogonal directions. We were also interested in testing the effect of array size on sensitivity for a variety of applications. Given those two considerations, and constraining our path to existing telecommunications conduits, we settled on a figure-eight path spanning two rectangles, one larger than the other, pictured in Figure 1 with channels color coded for easier comparison to data plots.

To achieve this geometry, there were two options: run new fiber, or splice existing fiber lines at many points. Due to the cost structure at this particular site, we chose the former. Over 2.5 km of fiber-optic cable was run in existing telecommunications conduits 1–2 m below the surface. The conduits are pipes roughly 10 cm in diameter, and in many locations the conduits are surrounded with cement slurry to protect them from digging. At the end of the first loop through the figure eight, two fibers in the same jacket are spliced end-to-end so that we can record

---

[1]Stanford University.
[2]OptaSense Inc.

signal at each location on both fibers simultaneously with an offset that effectively doubles our sensor density.

The interrogator unit (IU), an OptaSense ODH-3, sits in a secure server room where existing network infrastructure is used to easily plug in to the fiber network. The IU is configured to always run with a 7.14 m gauge length. Typically we record with passive settings with 8.16 m channel spacing at 50 samples per
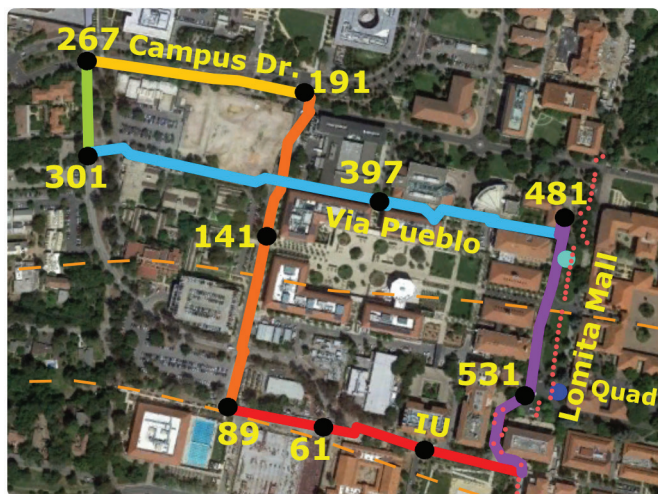

Figure 1. The fiber runs in a figure-eight shaped path, following two rectangular regions around campus, color coded for easy comparison with data plots. The longest straight segment is roughly 600 m. The fiber is spliced to itself at the end to follow the same path twice and effectively double the sensor density during passive recording. A subset of passive channels, numbered after interlacing traces from both fibers in the jacket, are marked for reference. The blue dots along Lomita Mall mark two of the betsy gun shots in the March 2017 active survey. Shot A (royal blue), shot B (cyan), and the small pink dots represent the 3C nodes in this region. The Stock Farm Monocline sits within the region outlined by the orange dotted lines. Nodes were deployed along Lomita Mall and continued along the same line toward the southwest.

second on 626 channels along both loops through the figure eight, which corresponds to 4.08 m effective channel spacing. Since the IU is stored in a server room, our data can continuously stream onto the computers where we perform analyses.

When we performed tap tests for spatial calibration and carried out the active-source survey, we needed denser, higher frequency sampling. On those designated days we switched to active settings: 1.02 m channel spacing at 2500 samples per second on 2480 channels spanning just the first loop through the figure eight. Active settings yield higher resolution, less-aliased data, but they generate roughly 2 TB of data per day, the same amount of data that passive settings generate in six months.

Active-source survey with DAS and nodes

Although direct comparisons of DAS and geophone data exist (Daley et al., 2013; Mateeva et al., 2013; Bona et al., 2017), most of this work has compared these systems in a downhole vertical seismic profiling environment, with fiber either cemented or clamped in place to ensure good coupling. There have been other active-source near-surface surveys using DAS (Dou et al., 2016; Lancelle, 2016), but these relied on cables buried in trenches so the fiber was directly coupled to the ground. Our system has complicating factors that we needed to compare to 3C geophones including:

- strong sensitivity to surface waves due to the horizontal array geometry,
- reduced coupling to the ground,
- and the ability of the fiber to slip in the conduit.

In March 2017, we recorded 37 betsy-gun sources and 81 four-fold sledgehammer source locations along Lomita Mall at Stanford University. Shots were continuously recorded on the DAS array and 82 3C geophones placed at 8 m spacing within 25 m east of the fiber. We also placed 16 nodes at 1 m spacing directly over a portion of the fiber, following a line parallel to Lomita Mall (Figure 1). The nodes were positioned to provide imagery of geologic structure under Stanford's main quad, and aligned approximately orthogonal to the Stock Farm Monocline (Kovach and Page, 1995).

When comparing the raw data, we would expect the difference of the inline component of neighboring 3C nodes spaced 8 m apart is most similar to the time derivative of a single DAS channel recorded at a 7.14 m gauge length and 1.02 m channel spacing. The response from betsy-gun sources A and B (mapped in Figure 1) on both DAS and nodes is plotted in Figures 2 and 3. The DAS data time derivatives are proportional to average
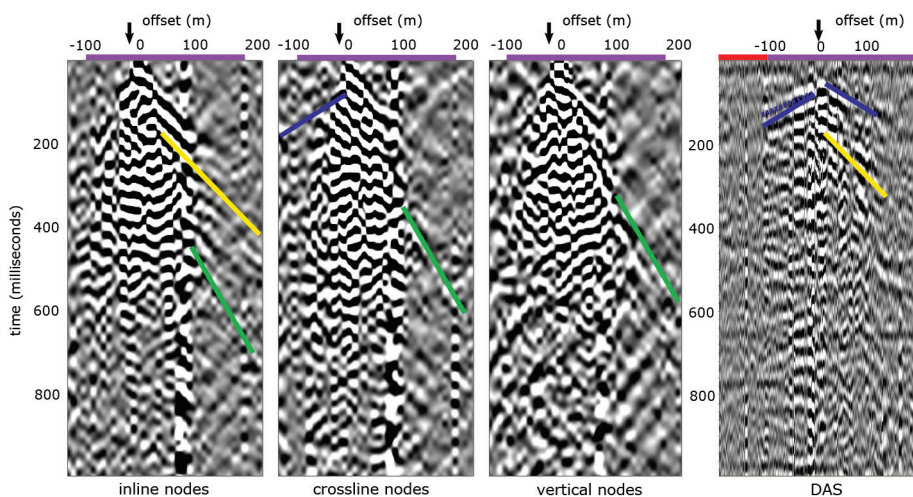

Figure 2. Records of shot A (from left to right) on the nodes' inline component, crossline component, vertical component, and DAS. Data were band-passed 2–40 Hz. To the right of the black arrows are sensors deployed straight along Lomita Mall, to the left of the arrows are sensors that curve between two buildings in the southeast corner of the DAS array starting around channel 531. The purple and red colors denote channels from Figure 1, so the red DAS channels head straight from the southeast corner of the array back toward the IU. A slow event is picked in green at 420 m/s, a bit fast for an airwave, but the lack of signal on the underground DAS suggests it is an airwave. The yellow line marks a 600 m/s event seen on both the inline nodes and DAS data (although the DAS event is really closer to 650 m/s). The solid dark blue lines denote an 1130 m/s event seen on the crossline nodes and DAS data. However, the DAS moveout to the south is closer to 1300 m/s, denoted by the dashed blue line (with solid for comparison).

Special Section: Fiber-optic distributed sensing

axial strain rate throughout each gauge length, which is similar to the difference of the inline particle velocities at the two ends of the gauge length. Based on the particular implementation of the optics, the detected source wavelet may be significantly altered (Bona et al., 2017), but we have not corrected for this in our data comparison.

As seen in Figures 2 and 3, both the 3C nodes (both the vertical and the inline-difference components) and the DAS array responded strongly to surface waves. We see some of the same events on the DAS and node data, several which appear to be refractions, particularly the fastest event seen in Figure 3 and possibly the fastest event seen in Figure 2.

There are clear practical advantages to using DAS for near-surface seismic imaging in urban areas. The fiber only requires a single standard AC power source, so there is no need to replace power sources in each sensor, which is particularly a concern in longer running surveys. In busy populated areas, the DAS array can easily be left in a secure conduit, while the nodes risk being moved or stolen and require field crew members to regularly check that nodes are present and functioning. The data from most node systems can only be examined after the survey is complete, so their quality cannot be checked between shots, but the DAS data are available shortly after recording.

In the southeastern corner of the DAS array, node placement was limited to small, irregularly scattered garden and tree plots because much of the surface is covered in cement, while the DAS followed a continuous conduit under the surface. This led to lower coherency in the node data than the DAS array in this region, as seen in Figures 2 and 3. The source of Figure 2 was closer to the southeast corner than that of Figure 3. However, this area of campus is particularly noisy, we believe due to waves bouncing between the basements of buildings on both sides of the fiber and node lines. Because the DAS array is underground, it does not record the airwave seen in the node data, highlighted

by a violet line in Figures 2 and 3. Additionally, surface waves showed less aliasing in the DAS data than in the nodes, particularly obvious in the slow airwave, due to the eight times increase in sensor density.

Although we found many operational advantages to using a DAS array, further processing and migration of the data will be necessary to understand whether the utility of such an array is constrained to refraction surveys, or if it is an acceptable tool for improving imaging of deeper reflections. Ultimately, the noise level in urban environments is the biggest challenge in processing these data.

Local weak earthquakes: Repeatability and kinematic analysis

In the previous section we observed strong anthropogenic noise recorded by our DAS array, particularly during the day. Therefore, the first-order question that our earthquake analysis aimed to answer is whether the events we observe in the recorded data correspond to actual seismic events or coherent nose generated locally on campus. We analyzed the repeatability of recordings corresponding to known events that occurred at approximately the same location and with presumably similar source mechanisms. Fortunately, we are in the vicinity (~14 km) of a quarry where dynamite blasts are generated on a weekly interval. The recording of quarry blasts is indeed repeatable, as shown by two examples in Biondi et al. (2017). Here we show the recording of an earthquake doublet occurring on Stanford's campus near Felt Lake, 4.2 km from the DAS. The distance between their epicenters was about 100 m, and they occurred one minute apart just before 1 p.m. local time.

To validate events observed in DAS data, we use the USGS earthquake online database and publicly available data recorded by a broadband seismometer at the Jasper Ridge Biological Preserve (JRSC station) that is managed by the Berkeley Digital Seismic Network. The Jasper Ridge station is located about 6.4 km from our DAS array. Because near-surface conditions are different below our array and JRSC, and the raypaths are different, the waveforms are not directly comparable. However, JRSC data provide a rough indication of the arrival time and relative strength of the signal corresponding to different arrivals (e.g., P-waves, S-waves, and surface waves). More recently, USGS has temporarily installed broadband seismometers within the DAS array area for more direct comparisons of timing for a small number of seismic events to mitigate the shortcomings of JRSC comparisons.

Figure 4 shows the data recorded by our DAS array and the Jasper Ridge Seismic Station's broadband seismometer corresponding to the first (magnitude 1.35) and second (magnitude
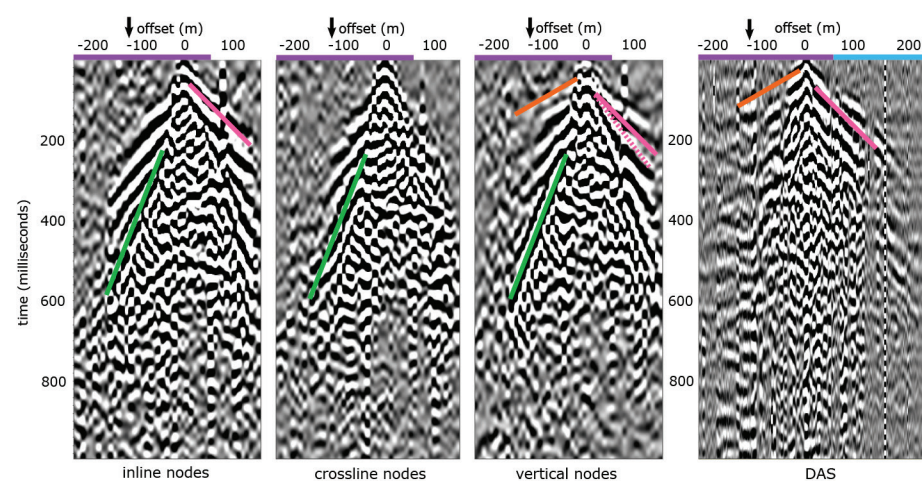

Figure 3. Records of shot B (from left to right) on the nodes' inline component, crossline component, vertical component, and DAS. Data were band-passed 2–40 Hz. To the left of the black arrows are sensors that curve between two buildings in the southeast corner of the DAS array. The sensors marked with a purple line to the right of the arrow are sensors deployed straight along Lomita Mall. Some nodes continue in a straight line farther north than the DAS array. Like in Figure 1, the channels marked with light blue are DAS channels heading northwest along Via Pueblo. A 350 m/s wave (airwave) annotated in green is visible on the nodes. A 1465 m/s wave is picked on both the DAS and vertical node data in orange. A 760 m/s wave is seen along the solid pink line on the DAS and inline node data, and shown for comparison to a 660 m/s event denoted by the dashed pink line on the vertical node data.

0.95) Felt Lake events on 12 July 2017. The DAS data were preprocessed via laser-noise attenuation, trace balancing, and band-passing from 0.25 to 12 Hz. The Jasper Ridge data were band-passed from 0.25 to 12 Hz as well. The Jasper Ridge Seismic Station is approximately the same distance from the epicenter as our DAS array but in a different direction, so the timing of the event arrivals should only be roughly similar. We use the convention that 0 s is the event time provided by USGS to set the origin of the time axis for all following earthquake data displays.

The DAS data shown in Figure 4 show strong and repeatable waveforms between both events across many parts of the array starting at about 3.7 s. These are likely to be a mix of S-waves and surface-wave arrivals. The waveforms are complex because of the complexity of the near surface both close to the epicenter and in the vicinity of the DAS array. However, they stand out from the strong background noise, including some noise due to vehicles passing along the array. As expected, the signal-to-noise ratio is higher for the first stronger event than the second weaker event. There is no clear P-wave arrival visible in either of the two DAS recordings. The P-waves arrived at Jasper Ridge after approximately 1.4 s, as is clearly observable from the vertical-component trace shown in Figure 4. The corresponding vertical-component trace in the second event of Figure 4 shows a weaker, but still identifiable, P-wave arrival.

The Felt Lake examples demonstrate the repeatability of signals recorded by the DAS array, but they do not show clearly identifiable P and S phases, due in a large part to strong ambient noise generated on campus. Figures 5 and 6 show that under quieter conditions we can clearly measure the kinematics of both P- and S-wave arrivals. Figure 5 shows the data recorded by our DAS array and by the broadband JRSC station around 3 p.m. local time during a magnitude 2.0 earthquake under Ladera, California, 3.8 km from the array. The data are displayed after laser-noise attenuation and band-passing from 0.25 to 20 Hz. The Jasper Ridge Seismic Station is much closer to this event, so the P-wave arrival is recorded by JRSC 0.5 s before it arrives at the DAS array. As in the previous example, the waveforms are complex due to subsurface scattering, but the P-wave arrival is clearly identifiable as reaching the DAS array around 1.5 s. Similarly the S-wave arrival is recorded at Jasper Ridge around 1.7 s and by the DAS array at 3 s.

The kinematics of both arrivals are more easily detected using the trace envelopes rather than oscillatory waveforms. Figure 6 shows the envelope of the DAS data shown in Figure 5. The time shifts within the array are consistent with an event arriving from the southwest direction and hitting the southwest corner of the array first: around channels 100 and 300. Unfortunately around channel 300, vehicles driving close to the array cause strong interfering noise.

All of these events are coming from southwest of the array, which explains why the southwest corners of the two rectangles in the array (around channels 100 and 310) tend to appear as event apexes. Throughout many earthquake recordings,
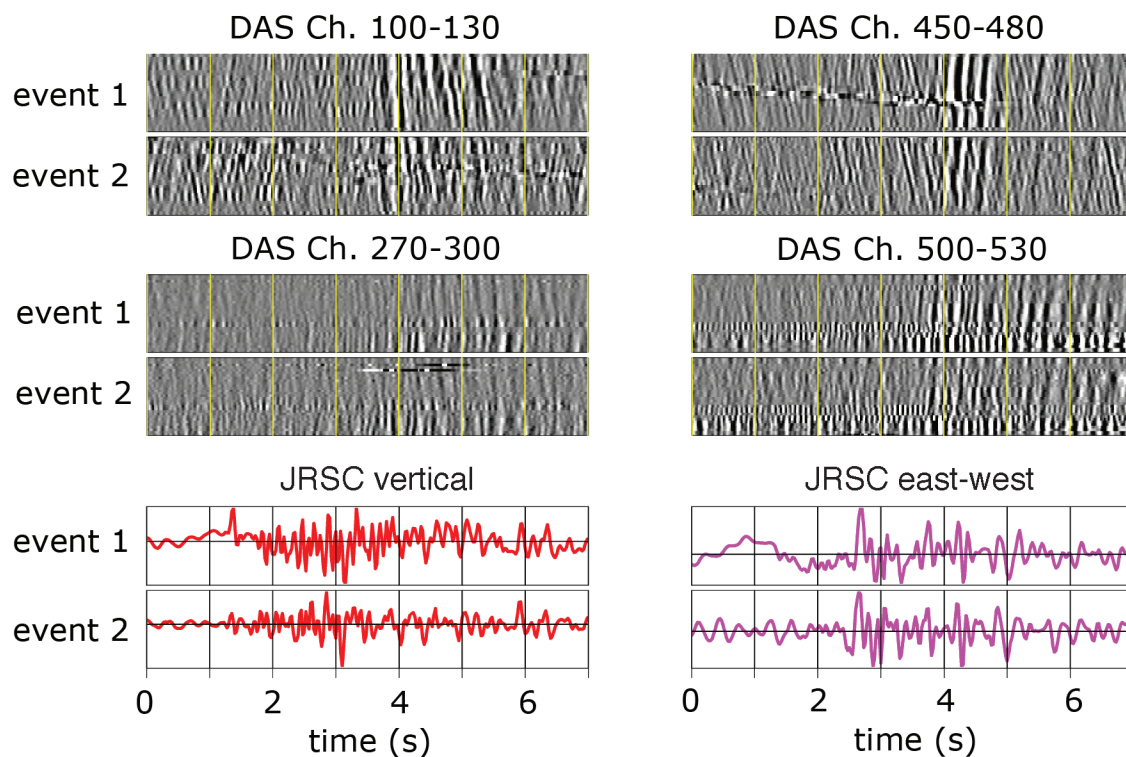

Figure 4. A comparison of the two Felt Lake earthquake events shows that their recordings on the DAS array (top two rows) are roughly as repeatable as their recordings on the Jasper Ridge Seismic Station broadband sensor (bottom row). Channel numbers increase going toward the bottom of each panel. There is some local noise including cars driving along the array (see event 2 along channels 100–130 and event 1 along channels 450–480) disrupting the repeatability, but moveouts during the event are roughly the same along straight segments of fiber. All data are band-passed from 0.25 to 12 Hz. The time-axis origin is the time of the event according to the USGS online database and channel numbers correspond to the markings on Figure 1.

including the Felt Lake events, we often see slow features traveling at a roughly constant velocity along each straight segment of the fiber. We are investigating these to determine whether they are recordings of waves propagating along the telecomm infrastructure or caused by near-surface scattering of surface waves.

Near-surface dispersion analysis from ambient-noise interferometry

For the purpose of cost-effective, easy near-surface characterization, we are interested in processing ambient noise to avoid the cost and time requirements involved in active surveys. Ambient-noise interferometry has been used successfully with point sensors to create data mimicking active surveys at the city scale (Chang et al., 2016) and time-lapse surveys at the reservoir scale (de Ridder, 2014). Passive Rayleigh-wave interferometry has been applied to trenched-fiber DAS data for imaging at geotechnical scales (Martin et al., 2016; Dou et al., 2017; Zeng et al., 2017), but this yields no information between lines in the array. Hoping to increase our ray coverage throughout the space between fiber lines, we calculated virtual-source response estimates for fiber channels throughout our 2D array.

We used six days of data from early April, including all 24 hours of the day. Even when averaging over multiple days of data, ambient-noise preprocessing decisions can cause significant biases in the estimated Green's functions retrieved by crosscorrelation (Fichtner, 2014). Thus, we did minimal preprocessing: data were divided into five minute windows with 50% overlap, were band-passed from 0.5–24 Hz, were set to their +/- 1 sign bit, crosscorrelated, then stacked for each hour. After saving each hour's average crosscorrelations throughout the week, we normalized the crosscorrelations by their L2 norms. Finally these virtual-source response estimates were stacked over six days, yielding a virtual-source response estimate.

We see the resulting crosscorrelation estimates for two virtual sources, channel 61 and 141 in Figure 7. We see strong responses from the channels collinear with the virtual sources. These continue to orthogonal channels nearby, but at a different apparent velocity and frequency content (for instance, channel 141's response on channels 320 to 390 between 0.1 and 0.5 s). There are also clear signals on channels parallel to the virtual sources: for channel 61, there is a strong response from channels 300 to 350 between 0.75 and 1 s. For channel 141, there is a weak response from channels 270 to 300 between 0.25 and 0.5 s. The estimated responses extracted from channels collinear with the virtual source are expected to yield Rayleigh waves, and channels directly across from each other along parallel lines primarily yield Love-wave responses, but other channel combinations can yield a mix of Love, Rayleigh, and converted waves (Martin and Biondi, 2017), so we are continuing to develop techniques to use these mixed modes.

We calculate Rayleigh-wave dispersion images from virtual-source response estimates limited to channels along the same line as these, as seen in Figure 8. These were calculated via tau-p transforms followed by a Fourier transform in tau. These dispersion images tell us how much energy is traveling at each velocity for a given frequency. At 5 Hz the main velocity

near channel 61 is 700 m/s, and such a wave would be sensitive to features in the top 45 to 70 m. Over at channel 141, the peak velocity for 5 Hz waves is closer to 400 m/s, which would be sensitive to features at a scale of 25 to 40 m. At both locations, the peak at 5 Hz continues down through and is likely the fundamental mode. At 10 Hz, the main velocity near channel 61 is around 400 m/s, which would be sensitive to features at a scale of roughly 13 to 20 m. Farther north, at channel 141, the peak velocity for 10 Hz is closer to 300 m/s, which would be sensitive to features in the top 10 to 15 m.
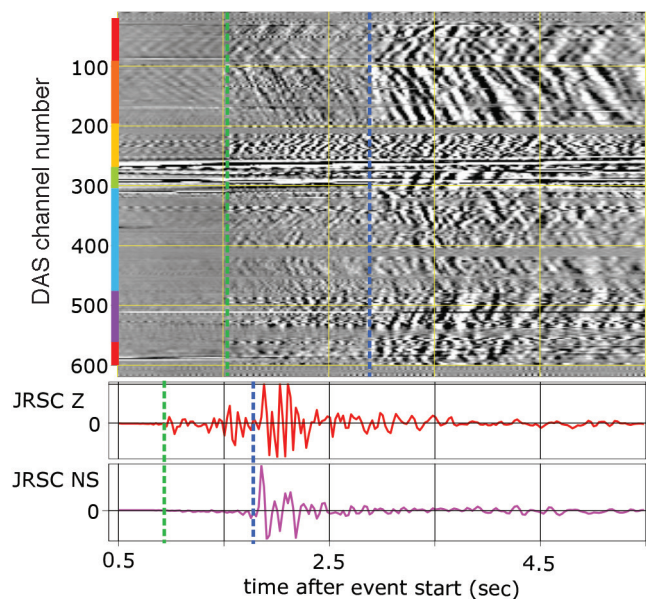

Figure 5. Top panel: DAS array recording for the Ladera earthquake. The time-axis origin is the time of the event according to USGS online database and channel numbers correspond to the markings on Figure 1. Middle panel: vertical component of the Jasper Ridge broadband seismometer. Bottom panel: north-south component of the Jasper Ridge broadband seismometer. Channels are colored according to Figure 1. All data are band-passed from .25 to 20 Hz. P-wave arrivals (green) and S-wave arrivals (blue) are picked for each location, but the broadband is several miles from the DAS array, so timing is not the same.
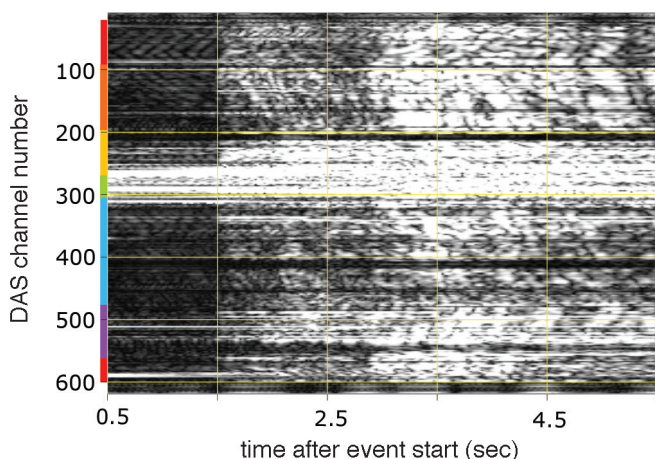

Figure 6. Envelope of the DAS array data recorded for the Ladera earthquake. The time-axis origin is the time of the event according to USGS online database and channel numbers and colors correspond to the markings on Figure 1. Data are band-passed from 0.25 to 20 Hz.

For earthquake hazard analysis, engineers must estimate surface-wave and S-wave velocity in the top 30 m of the subsurface. Thus, the frequencies at which we extract signals are in the right range for geotechnical studies, and the ability to cut the cost of these surveys could enable more widespread near-surface stability studies.

Our convergence analysis indicates that just four days of data are enough to yield stable virtual-source response estimates when compared to estimates from the same full month of data. But data collected from November through April yielded higher signal-to-noise ratios at longer distances than data in September and October. This can be seen comparing Figures 7 and 8, the virtual-source response estimates to the same channels in September, shown in Martin and Biondi (2017). While one possible explanation may be saturation-related near-surface changes, further quantitative analysis is needed to determine causes of virtual-source response estimate changes on a campus with many transient-noise sources. Even for static virtual-source

response estimates, the issues of preprocessing related biases are especially pertinent in environments with transient-noise sources, so we are working toward scalable methods for automatic identification and filtering of these sources in urban environments (Huot et al., 2017).

Potential future applications

The economic advantages of recording seismic using fiber cable in open conduits, either by using "dark fibers" or newly deployed fiber cables, make this recording technology appealing for many future applications. However, the characteristics of the data recorded by such a configuration will require the development of novel processing and imaging algorithms.

This new type of seismic acquisition opens the door to a variety of cost-effective installation types: (1) permanently recording sections in targeted, potentially large areas of interest, (2) quickly plugging into fiber to create a dense, on-demand array, (3) reconfigurable arrays that can be revisited months or
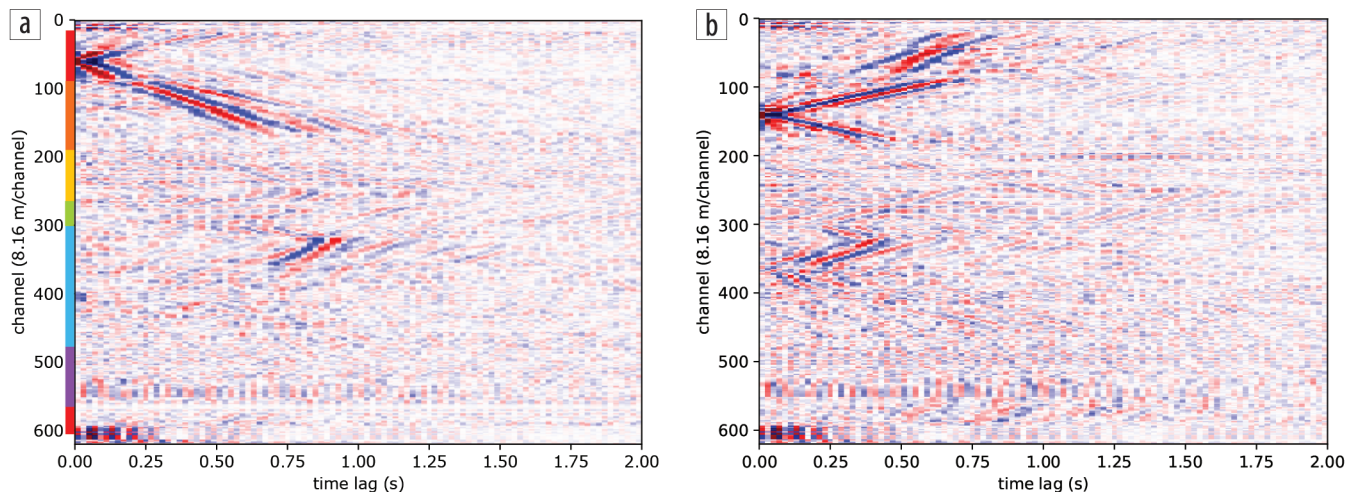

Figure 7. Symmetrized virtual-source response estimates for (a) channel 61 and (b) channel 141 throughout the array show clear signals extracted from channels collinear with the virtual sources, channels parallel to the virtual sources, and channels orthogonal to the virtual sources. Channel spacing is 8.16 m, but with the second loop through, it is effectively 4.08 m. In the left panel, channels are marked by their color from Figure 1.
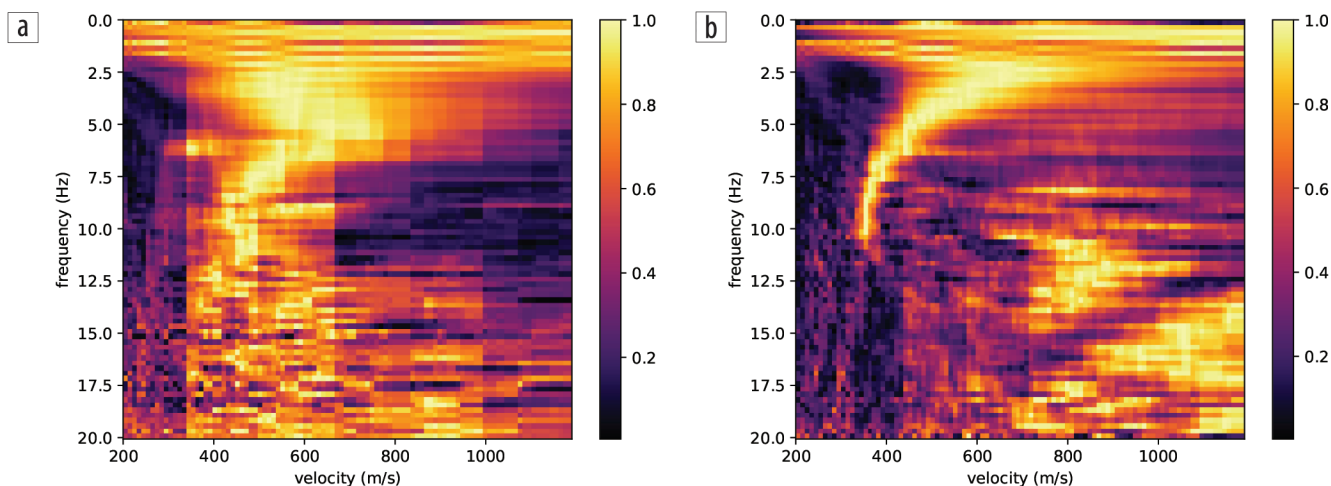

Figure 8. We calculated Rayleigh-wave dispersion images from the channels inline with virtual sources at (a) channel 61 and (b) channel 141. For each frequency the dispersion values are normalized so the peak velocity point is 1.0. The fundamental mode for channel 141 is particularly clear.

Special Section: Fiber-optic distributed sensing

years later with repeatable receiver geometry. There is a great deal of scientific discovery that may be enabled by dense, wide-aperture array for continuous or on-demand monitoring of seismically active regions.

In the energy industry, this technology would be ideal for regional-scale induced seismicity monitoring, particularly in areas where there is little history of significant naturally occurring seismicity. The data might be used for earthquake hazard analysis and potentially even for early earthquake warning. Such a system could be reconfigured over time to follow areas experiencing an uptick in seismicity or which have new production activities planned.

Summary

We have been continuously recording seismic data on a DAS array deployed in existing telecommunications conduits underneath the Stanford University campus since September 2016. These data are being analyzed for multiple purposes including an active-source survey with a 3C node comparison, earthquake detection and characterization, and continuous interferometric imaging of the near surface. Despite some loss in sensitivity relative to DAS arrays directly coupled to the soil, we have been able to record surface waves and refractions from an active survey, detect small repeatable nearby earthquakes, and extract coherent virtual-source response estimates from ambient noise. These findings show promise for a scalable new method for long-term seismic acquisition. **TLE**

Acknowledgments

Corresponding author: ermartin@sep.stanford.edu

References

Biondi, B. L., E. R. Martin, S. Cole, M. Karrenbach, and N. Lindsey, 2017, Earthquakes analysis using data recorded by the Stanford DAS array: 87th Annual International Meeting, SEG, Expanded Abstracts, 2752–2756, https://doi.org/10.1190/segam2017-17745041.1.

Bona, A., T. Dean, J. Correa, R. Pevzner, K. V. Tertyshnikov, and L. Van Zaanen, 2017, Amplitude and phase response of DAS receivers: 79th Conference and Exhibition, EAGE, Extended Abstracts, https://doi.org/10.3997/2214-4609.201701200.

Chang, J. P., S. A. L. de Ridder, and B. L. Biondi, 2016, High-frequency Rayleigh-wave tomography using traffic noise from Long Beach, California: Geophysics, **81**, no. 2, B43–B53, https://doi.org/10.1190/geo2015-0415.1.

Daley, T. M., B. M. Freifeld, J. Ajo-Franklin, S. Dou, R. Pevzner, V. Shulakova, S. Kashikar, D. E. Miller, J. Goetz, J. Henninges, and S. Lueth, 2013, Field testing of fiber-optic distributed acoustic sensing (DAS) for subsurface seismic monitoring: The Leading Edge, **32**, no. 6, 699–706, https://doi.org/10.1190/tle32060699.1.

de Ridder, S. A. L., 2014, Passive seismic surface-wave interferometry for reservoir-scale imaging: PhD thesis, Stanford University.

Dou, S., J. Ajo-Franklin, T. Daley, M. Robertson, T. Wood, B. Freifeld, R. Pevzner, J. Correa, K. Tertyshnikov, M. Urosevic, and B. Gurevich, 2016, Surface orbital vibrator (SOV) and fiber-optic DAS: Field demonstration of economical, continuous-land seismic time-lapse monitoring from the Australian CO2CRC Otway site: 86th Annual International Meeting, SEG, Expanded Abstracts, 5552–5556, https://doi.org/10.1190/segam2016-13974161.1.

Dou, S., N. Lindsey, A. M. Wagner, T. M. Daley, B. Freifeld, M. Robertson, J. Peterson, C. Ulrich, E. R. Martin, and J. B. Ajo-Franklin, 2017, Distributed acoustic sensing for seismic monitoring of the near surface: A traffic-noise interferometry case study: Scientific Reports, **7**, no. 1, https://doi.org/10.1038/s41598-017-11986-4.

Fichtner, A., 2014, Source and processing effects on noise correlations: Geophysical Journal International, **197**, no. 3, 1527–1531, https://doi.org/10.1093/gji/ggu093.

Huot, F., Y. Ma, R. Cieplicki, E. Martin, and B. Biondi, 2017, Automatic noise exploration in urban areas: 87th Annual International Meeting, SEG, Expanded Abstracts, 5027–5032, https://doi.org/10.1190/segam2017-17774369.1.

Kovach, R. L., and B. M. Page, 1995, Seismotectonics near Stanford University: California Geology, **48**, no. 8, 91–98.

Lancelle, C., 2016, Distributed acoustic sensing for imaging near-surface geology and monitoring traffic at Garner Valley, California: PhD thesis, University of Wisconsin.

Martin, E. R., N. J. Lindsey, S. Dou, J. Ajo-Franklin, T. M. Daley, B. Freifeld, M. Robertson, C. Ulrich, A. Wagner, and K. Bjella, 2016, Interferometry of a roadside DAS array in Fairbanks, AK: 86th Annual International Meeting, SEG, Expanded Abstracts, 2725–2729, https://doi.org/10.1190/segam2016-13963708.1.

Martin, E. R., and B. L. Biondi, 2017, Ambient noise interferometry across two-dimensional DAS arrays: 87th Annual International Meeting, SEG, Expanded Abstracts, 2642–2646, https://doi.org/10.1190/segam2017-17677759.1.

Mateeva, A., J. Lopez, J. Mestayer, P. Wills, B. Cox, D. Kiyashchenko, Z. Yang, W. Berlang, R. Detomo, and S. Grandi, 2013, Distributed acoustic sensing for reservoir monitoring with VSP: The Leading Edge, **32**, no. 10, 1278–1283, https://doi.org/10.1190/tle32101278.1.

Zeng, X., C. Thurber, H. Wang, D. Fratta, E. Matzel, and PoroTomo Team, 2017, High-resolution shallow structure revealed with ambient noise tomography on a dense array: Presented at 42nd Workshop on Geothermal Reservoir Engineering, Stanford University.